ORIGINAL PAPER

MECHANICAL AND TRIBOLOGICAL PROPERTIES OF BREAK PAD MATERIALS USING RECYCLED STYRENE-BUTADIENE RUBBER AND WOOD DUST

CAMELIA PINCA-BRETOTEAN [1], ANA JOSAN [1], SORIN AUREL RATIU[1], CORNELIU BIRTOK-BANEASA[1]

Manuscript received: 11.10.2025; Accepted paper: 30.11.2025; Published online: 30.12.2025.

Abstract. *The growing interest in sustainable friction materials is driven by concerns about the environmental and human health impacts of conventional brake pad compositions. The work aims to develop and characterize friction materials with a high content of recycled and natural components. The paper will evaluate the mechanical, tribological, and thermal stability performances of the sustainable friction materials for brake pads used for medium-performance urban vehicles. The materials were made according to three recipes containing recycled styrene-butadiene rubber (SRB) from used tires, sawdust, graphite, barite, iron oxide, zirconium oxide, and Novolac phenolic resin treated with hexamethyltetramine. The three recipes were made with different volume fractions of rubber and sawdust, the concentration of the other components in the recipes being kept constant. The materials were made by cold pressing and sintering. Density, hardness, porosity, compressive strength, elongation, resilience, pin-on-disc tribological tests, and thermal stability evaluations were performed. The proposed material is a viable, sustainable, and efficient alternative for light braking applications*

Keywords: *Resin; styrene-butadiene rubber; sawdust; friction; pad.*

1. INTRODUCTION

Brakes are essential components of motor vehicles due to performance and passenger safety considerations [1]. The braking operation occurs as a result of the driver applying pressure to the brake pedal. As a result of this mechanical action, friction forces arise at the interface between the brake pads and the disc/drum. They reduce the rotational movement of the disc/drum and the axle on which they are mounted, slowing the vehicle down to a stop. The friction between the disc/drum and the brake pad causes wear of the materials on the surface of these components. As a result, the thickness of the brake pad is reduced, and the distance between the disc/drum and it increases. This leads to a decrease in braking performance [2].

Regarding passenger safety during braking, it is strongly influenced by the correct functioning of the braking system, which depends on the contact interface between the pad-disc/drum [1]. When braking problems occur, the main cause is always due to the brake pads, generated by the following factors: vehicle speed, pedal pressure, temperature, environmental conditions, and their durability [3]. The brake disc/drum is responsible for the occurrence of

[1]University Politehnica Timișoara, Faculty of Engineering Hunedoara, Department of Engineering and Management, 331028 Hunedoara, Romania. E-mail: camelia.bretotean@fih.upt.ro.

https://doi.org/10.46939/J.Sci.Arts-25.4-b02

vibrations and noise during vehicle operation. On the other hand, as a result of the wear process during braking, fine particles are released into the atmosphere that are harmful to the environment and human health [4]. Braking wear and particles emitted into the atmosphere are correlated with vehicle driving behavior, frequency and intensity of braking, brake pad type, and road surface type [5]. At the beginning of braking, the wear process generates large particles in the atmosphere, which subsequently decrease in size when stable contact is formed between the brake pad surface and the disc/drum [6]. In the specialized literature, works have been published on wear particles released into the atmosphere. The conclusions of these studies show that the most important metal pollutants are: copper, cadmium, nickel, lead, antimony, and zinc [7]. In this context, the environmental and human health impact of particles generated by the braking process are important criteria in the selection and development of friction materials intended for the production of brake pads for motor vehicles. Thus, in the automotive field, the transition to ecological practices is not only a condition imposed by European regulations, but also a transition to a more economically viable environment, which is a significant boost for the use of sustainable materials. This contributes to reducing greenhouse gas emissions and conserving natural resources, with a reduced impact on the environment. Many of the sustainable materials are lighter than traditional ones, which means reducing the weight of vehicles, with effects on reducing fuel consumption and carbon emissions. These materials are by-products resulting from various human activities. In the production of eco-friendly brake pads, natural fibers and particles exhibit unique characteristics when interacting with other materials [8]. Currently, natural fibers are preferred over traditional synthetic fibers because they offer a wide range of advantages, such as environmental protection, regenerability, low cost, low density, and superior mechanical properties [9]. In the literature, there are works that have studied friction materials for brake pads from ecological and sustainable sources.

Wang et al. [10] developed resin-based friction materials with hybrid fibers: wood and rockwool in a proportion of 30%. Studies have shown that as wood fiber increases, density and hardness decrease, but wear resistance improves. The optimal composition of 5% wood and 25% rockwool provided friction coefficients and thermal stability [10].

Kurniawan et al. manufactured brake pads from teak wood powder, rice ash and epoxy resin, aluminum, and magnesium by applying sintering technology at 180^0C. The conclusions of the paper show that the application of hot pressing led to improvements in hardness, wear, and braking distance values [11].

Nandiyanto et al. investigated the possibility of using sawdust in the automotive industry to build environmentally friendly brake pads with superior performance. Experimental results demonstrate that the strength of brake pads is influenced by the difference in composition between sawdust and resin [12].

Dirisu et al. are conducting studies on the use of natural fibers in brake pads as an alternative to harmful asbestos-based materials. Thus, in the manufacture of friction materials, agricultural waste (coconut shell and oilseed stalk) was used as filler elements, along with industrial waste from metal chips. The developed brake pads performed favorably compared to existing commercial brake pads [13].

Tamayo et al. studied brake pads manufactured with rubber particles from recycled tires, analyzing tribological and wear properties. The conclusions of the study show that increasing the size of ground rubber particles leads to a decrease in the friction coefficient of the friction material [14].

The work aims to produce and characterize in the laboratory friction materials with a high content of recycled and natural components. The paper will evaluate the mechanical, tribological, and thermal stability of the sustainable friction materials for brake pads used for medium-performance urban vehicles. The paper analyzed three friction material recipes

containing recycled styrene-butadiene rubber (Styrene-Butadiene Rubber-SRB) from used tires, oak sawdust, graphite, barite, iron oxide, zirconium oxide, and Novolac-type phenolic resin treated with hexamethyltetramine. The three recipes were made with different volume fractions of rubber and sawdust, the concentration of the other components in the recipes being kept constant.

2. MATERIALS AND METHODS

The production of friction materials for brake pads was based on the analysis of the role of each material chosen in the composition of the recipes.

2.1. MATERIALS

SRB is a synthetic rubber resulting from the copolymerization of styrene (C_8H_8), which provides hardness and adhesion, and butadiene (C_4H_6), which provides elasticity and flexibility. This type of rubber used in the recipes is obtained by grinding used tires, taken from different parts of the tire, inner lining, tread, and sidewalls. In the composition of the recipes, rubber is obtained by fine grinding at ambient temperature, resulting in a powder with a granulation of 100μm. This is a filler material that acts as a noise and vibration dampener and provides elasticity and flexibility to the structure of the composite material. Sawdust is an organic material with a partial role as filler and reinforcement. This is a hardwood component due to its high lignin content, which makes it more heat-resistant than softwood sawdust. The advantages of including it in the recipe are that it improves friction stability at moderate temperatures, is an environmentally friendly, biodegradable material, and contributes to the absorption of noise and vibrations. However, sawdust begins to lose structural integrity at temperatures above 200°C. Thus, the friction material is recommended for light vehicles with a medium braking regime, intended for urban use. To improve structural integrity, a heat-resistant Novolac phenolic resin base was used. The sawdust was sun-dried for three weeks after collection. This was ground in a ball mill and then sieved through sieves of various sizes. The final granulation is rigorously controlled, the granulometry being maintained below 0.1 mm (Figure 1).

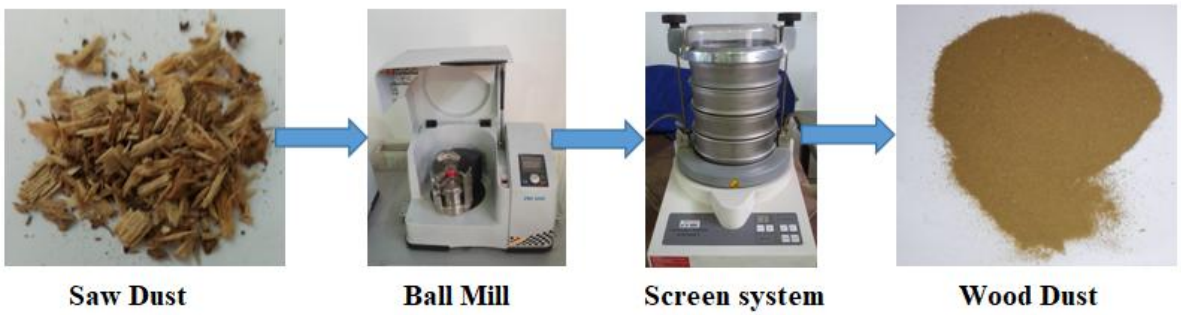

Figure 1. Sawdust used in the production of composites.

The chemical composition of the sawdust used in the production of friction material is presented in Table 1.

Table 1. Chemical composition of oak sawdust.

Cellulose [%wt]	Hemicellulose [%wt]	Lignin [%wt]	Resins [%wt]	Ash [%wt]	Water [%wt]
45.26	20.83	25.11	3.4	0.9	4.5

Table 1 shows that sawdust has a high cellulose content, which gives strength and fibrousness to the composite material. Hemicellulose contributes to achieving good cohesion between the components of the composite material, but is susceptible to thermal degradation. Lignin is an amorphous, heat-resistant aromatic polymer that imparts rigidity and increased chemical resistance to the composite materials. Ash mainly includes calcium oxides and traces of mineral salts that provide dimensional stability and adjust friction. The resins in oak sawdust have antioxidant properties and provide chemical stabilization to the composition, being beneficial in friction applications. The phenolic resin (Novolac type) is a thermosetting binder that transfers charge between particles, influencing hardness and thermal stability. This is being treated with hexamethylenetetramine as a hardener. Graphite is a solid lubricant with a wear-reducing role, thermally stable, and with properties to reduce the fluctuating friction coefficient. Iron oxide stabilizes friction and has a moderate abrasive effect. Barite is a dense filler that provides dimensional stability, adjusts friction, and zirconium oxide contributes to the hardening of the composite and ensures its thermal stability. Table 2 presents the chemical composition of the friction materials analyzed in this work.

Table 2. The composition of the friction materials.

Sample	SBR [%wt]	Wood dust [%wt]	Phenolic resin [%wt]	Graphite [%wt]	Iron oxide [%wt]	Barite [%wt]	Zirconiu oxide [%]	Total [%]
A5/30	5	30	20	10	15	12	8	100
A10/25	10	25	20	10	15	12	8	100
A15/20	15	20	20	10	15	12	8	100

The processing methodology consisted of mixing the components in powder form in a mixer, after which the phenolic resin was introduced. Mixing was continued for 15 minutes to obtain a homogeneous state of the raw material. The mixture was transferred into molds, designed and made of stainless steel. These are based on the characteristics of the experimental facilities available for carrying out composite material characterization tests. Fig. 3 shows the mold that allows obtaining samples for determining physical-mechanical characteristics, and Fig. 4 shows the mold for producing the pins necessary for performing tribological tests.

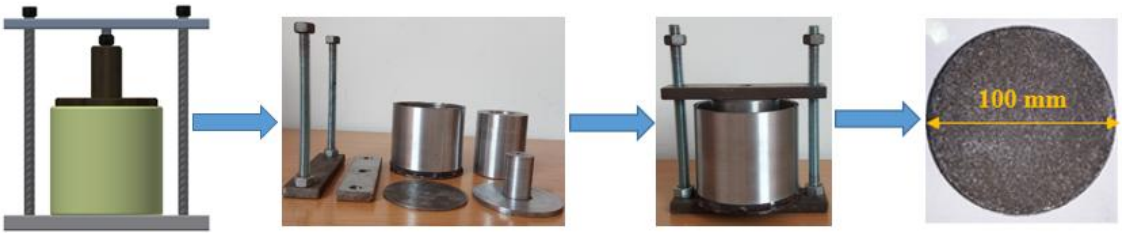

Figure 3. The mold for obtaining samples for determining physical and mechanical characteristics.

Figure 4. The mold for obtaining samples for assessing tribological behavior.

The mixture was uniaxially pressed into molds at a pressure of 150 bars for 1 minute at ambient temperature. The pressing was done in a hydraulic press of original design, shown in Fig. 5. After compaction, the molds were placed in an oven at 150°C for 6 hours, after which they were allowed to cool to ambient temperature for 12 hours. Subsequently, the mixture was subjected to a post-curing treatment at 170°C for one hour in a conventional oven (Fig. 6). The choice of this temperature was made to avoid degradation of rubber particles and pyrolysis of hemicellulose and lignin, processes that occur at temperatures higher than 200°C. At the end of the processing operation, the molds were left at room temperature for 24 hours, after which the samples were extracted.

Figure 5. Hydraulic press of original design.

Figure 6. Conventional oven type Nabertherm.

From the disk samples resulting from the mold shown in Fig. 3, parallelepiped samples with dimensions of 20x20x30 mm were made. These samples were used to determine the mechanical characteristics of the composite materials. The pins made with the mold shown in Fig. 4 were used to evaluate the tribological characteristics of the friction materials. To determine the wear characteristics, cast iron discs were developed in the laboratory with a chemical composition as close as possible to that of the brake discs currently produced, according to the standards in force (Fig. 7).

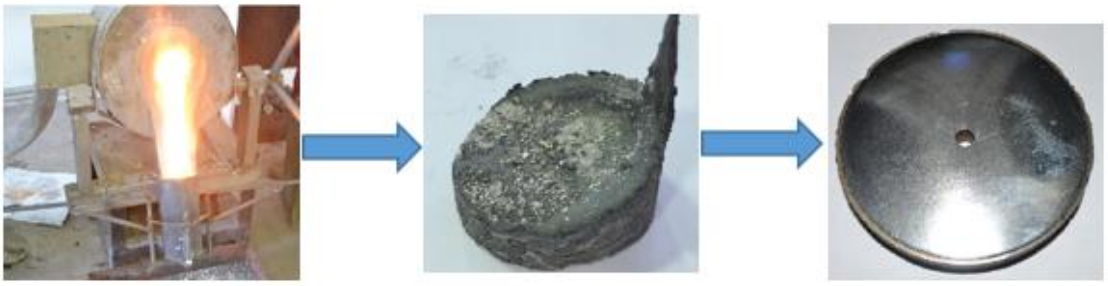

Figure 7. Production of cast iron discs used in tribological tests.

The chemical composition, density, and hardness of the cast iron resulting from the development under laboratory conditions are presented in Table 3.

Table 3. Chemical composition of laboratory-produced cast iron compared to ASTM A 159 standard.

Cast iron type	C %	Si %	Mn %	P %	S %	Density (g/cm^3)	HB
Laboratory cast iron disc	3.29	2.47	0.8	0.19	0.17	7.2	220
Standard ASTM A159 (G 2500)	3.2-3.5	2-2.4	0.6-0.9	0.2	0.15	6.9 – 7.3	170-229

The cast iron developed in the laboratory falls under the G 2500 brand, intended for the production of brake discs for vehicles.

2.2. METHODS

The density of the samples was determined by applying Archimedes' method by displacing water in a graduated cylinder (Fig. 8). For this purpose, the samples were weighed with an analytical balance, and the density of each composite material sample was determined with the relationship:

$$\rho = \frac{m}{V_f - V_i} \tag{1}$$

where: m - the mass of the composite material sample (g), V_i - the initial volume of water in the graduated cylinder (cm^3), and V_f - the final volume of water in the graduated cylinder after the sample is introduced (cm^3). Density determination was performed on parallelepiped samples with dimensions of 20x20x30mm. The final density was determined for five samples made from each composite material.

The porosity of the friction material was determined in oil, on parallelepiped samples with dimensions of 20x20x30 mm, made by cutting from the disk samples obtained with the mold shown in Fig. 3. These were weighed, determining the initial mass (M_i) then they were placed in a pot of heated oil to a temperature of 90°C ± 10°C and maintained at this temperature for 8 hours; the samples were removed from the pot and rolled on a cloth, to remove the excess oil; after performing this procedure, the samples were weighed again, noting their mass, (M_f). The porosity was determined with the relationship:

$$Porozity(\%) = \frac{M_f - M_i}{M_i} \cdot 100 \tag{2}$$

To determine the porosity for each composite material recipe, three determinations were performed, the final porosity being the arithmetic mean of them. Fig. 9 shows the samples prepared for porosity tests.

Figure 8. Aspects of density determinations.

Figure 9. Set of samples for porosity tests.

Figure 10. Compression test.

The hardness of the composite sample was measured using a Shore D hardness tester, according to ASTM D2240 (Shore D). The determination of compressive strength was carried out according to ASTM D695, the determination of tensile strength according to ASTM D638, and the elongation at break according to ASTM E8. The experiments were carried out on a Zwick/Roell Z050 universal testing machine, on a sample of eight specimens made from each material recipe, and for each mechanical characteristic, Fig. 10. Resilience was determined according to ASTM D256 on an Instron CEAST 9050 Charpy pendulum hammer.

The tribological characterization of friction materials was carried out in two stages. In the first stage, tests were carried out to determine mass wear, relative wear durability, and wear rate. In the second stage, the evolution of the friction coefficients was studied. Before any tribological test, all samples were subjected to a polishing process using SiC paper to obtain similar surfaces. The determination of mass wear, relative wear durability, and wear rate was carried out by the gravimetric method (weight loss), on an originally designed laboratory facility operating based on the pin-on-disc technique, in dry friction mode, shown in Figure 11. The principle of these tests consisted of loading the arm of the installation with 15N weights that press the pins made from the three recipes onto a cast iron disk.

Figure 11. Installation for determining the wear rate.

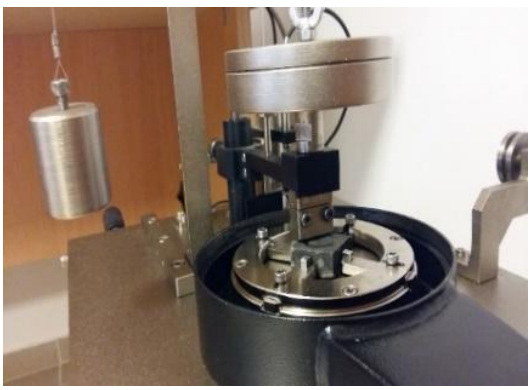

Figure 12. Installation for determining the coefficient of friction.

The rotating disk of the installation is made of cast iron produced in the laboratory and assimilated according to the ASTM A 159 standard with G 2500. The main parameters used in the tribological experiments are presented in Table 4.

Table 4. Parameters used in determining mass wear, relative wear durability, and wear rate.

Sliding speed v [m/s]	Force range R [mm]	Distance during wear L_u [m]	Trial time t_1 [min]
3.92	25	2000	8.5

Mass wear (u) was determined with the relationship [17]:

$$u = m_0 - m_f \tag{3}$$

where: m_0 - the mass of the specimen before the test (g), and m_f is the mass of the specimen after the test (g).

The relative wear durability was calculated by relating the mass wear of the composite material specimen (u_c) to the mass wear of the cast iron specimen (u_f), with the relationship [17]:

$$u_r = \frac{u_{castiron}}{u_{compozit}} \tag{4}$$

The wear rate was calculated based on the relationship [17]:

$$W = \frac{V}{F \cdot L} \tag{5}$$

where: V - the volume of material lost through friction (mm^3), F - the applied force (N), and L - the sliding distance (m).

At the end of the tests, the temperature in the contact area of the friction couplings (cast iron disc-organic composite material pin) was determined using a FLIR "Therma CAM Quick View" thermographic camera.

The determination of the friction coefficient was carried out using a TR-20 tribometer whose operating principle is based on the pin-on-disc technique. The equipment allows the mounting of specimens made of composite materials of parallelepiped shape with dimensions of 20x20x30 mm. The pin of the equipment is a steel ball with a diameter of 6 mm, and the friction regime used for the test is dry friction. During each test, the values of the friction coefficient were recorded continuously. The tests were performed at an ambient temperature of 22 ± 3°C, and the humidity was 22%. During the tests, a load of 15 N was applied, and the test parameters used in the experiment are presented in Table 5.

Table 5. Parameters for determining the evolution of the friction coefficient.

Wear mark diameter D [mm]	Speed n [rpm]	Testing time t_2 [s]	Average pressure p [N/mm^2]
15	150	18000	0,53

Fig. 12 shows the installation for determining the evolution of the friction coefficient.

3. RESULTS AND DISCUSSION

3.1. RESULTS

The mechanical characteristics of the composite materials produced in the laboratory are presented in Table 6. The densities of the materials, presented in Table 6, are low due to the incorporation of rubber particles, which have lower densities compared to the other components of the recipes.

Table 6. Physical and mechanical characteristics of friction materials.

Sample	Density [g/cm^3]	Porosity [%]	Hardness Sh [D]	Compressive strength [MPa]	Elongation [%]	Young's modulus (GPa)	Resilience (kJ/m^2)
A5/30	2.71	9	85	105	1.1	5.0	3
A10/25	2.49	11	72	87	1.5	4.3	5
A15/20	2.31	15	65	75	1.8	3.8	8

Porosity increased progressively with the amount of SRB. This increase was more pronounced at concentrations of 15% rubber. This is explained by the fact that SRB contains additives, oils, and cross-linked polymers that partially decompose at the temperatures of the manufacturing process. This degradation releases volatile gases (CO_2, H_2O, volatile organic compounds) that cannot be completely evacuated and generates micro- and macropores in the composite mass. On the other hand, the elastic rubber particles deform and partially return after the pressure is released, which prevents uniform compaction and causes the formation of voids between the phases.

Table 6 shows that with increasing porosity, the compressive strength decreases. This is explained by the reduction of the effective resistance section, the appearance of stress concentrators at the pore edges, the low adhesion at the phase interface, and the elastic behavior of the rubber particles, which prevents the uniform transfer of stresses. Overall, these effects lead to a less rigid structure and a decrease in the load-bearing capacity of the composite.

Hardness decreases with increasing SRB rubber, which is a soft material and decreases when wood dust is reduced. On the one hand, wood dust stiffens the matrix, and on the other hand, it increases porosity.

In [15], the authors reported that by adding between 5% and 15% by weight of rubber particles, both the hardness and density of the plates decreased, while the porosity increased. Similar conclusions were obtained in the present study.

Increasing the amount of SRB rubber improves the deformation capacity and energy absorption, due to the elastomeric nature of the rubber phase. SRB particles behave as deformable zones that redistribute stresses and dissipate mechanical energy through elastic deformation and internal friction mechanisms. In addition, they contribute to stopping crack propagation, leading to more tenacious behavior and improved resilience of the composite.
Stiffness decreases as the proportion of rubber increases. The decrease in the stiffness of the composite with increasing SRB content is explained by the reduced elastic modulus of the elastomeric phase, the increase in porosity, and the limited adhesion between the rubber and the phenolic matrix. SRB particles, having pronounced elastic behavior, favor the overall deformation of the material and reduce its ability to resist deformation. As a result, the composite becomes more flexible but less structurally rigid.

Based on relations 3, 4, and 5, presented in subchapter 2, the wear parameters were determined, the results being presented in Table 7.

Table 7. Wear parameters.

Sample	Wear mass [g]	Relative wear durability	Removed volume [mm^3]	Wear rate W [mm^3/Nm]
Cast iron disc	0.232	-	32.222	0.001074
A5/30	1.621	0.143	589.154	0.019638
A10/25	0.972	0.238	390.361	0.013012
A15/20	0.513	0.452	222.077	0.007402

For each recipe, the temperature was monitored throughout the tests. It was observed that at the beginning of the tests, until the distance of 500 m was covered, a rapid increase in temperature occurred in the area of the friction couplings. It is noted that for no sample did the temperature exceed 180°C. This was followed by a period of temperature stabilization, in the range of 500–1500 m, after which it began to decrease. This is explained by the fact that the temperature dissipates from the area of the friction couplings. The decrease in temperature in the contact area shows that the heat resulting from the friction process is dissipated, so there is less degradation of the organic components in the composite materials. For each recipe, the temperature at the end of the tests is presented in Fig. 13.

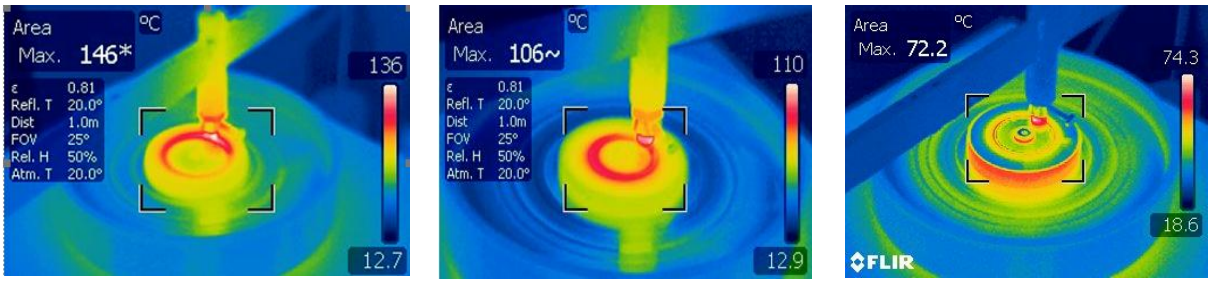

A5/30 **A10/25** **A15/20**

Figure 13. Temperatures in the area of the friction couplings at the end of the experiments.

Figs. 14–16, respectively, show the evolution of the friction coefficient for the three friction materials produced in the laboratory.

The variation of the friction coefficient at the beginning of the experiments is due to the irregularities of the surfaces of the friction couplings in contact. After a certain time from the beginning of the tests, as a result of the increase in the contact surface between the samples and the steel ball, the friction coefficient increased for all the tested samples.

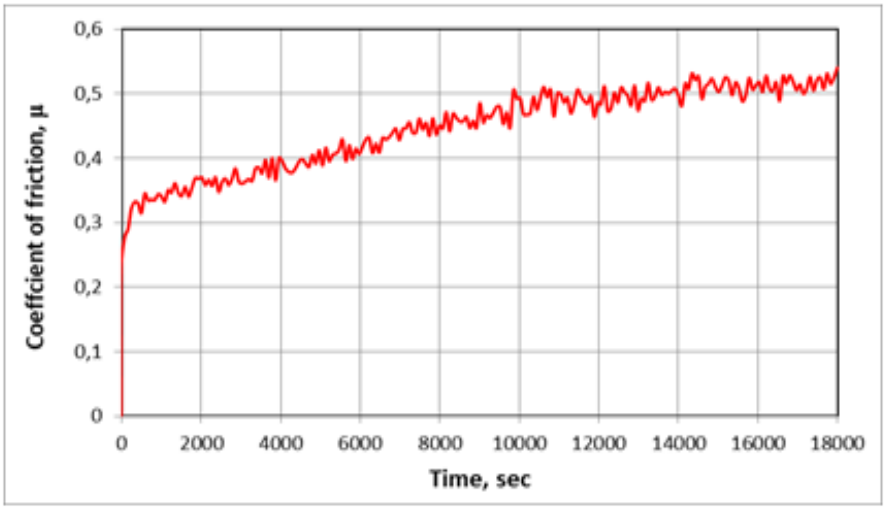

Figure 14. Evolution of the friction coefficient for sample A5/30.

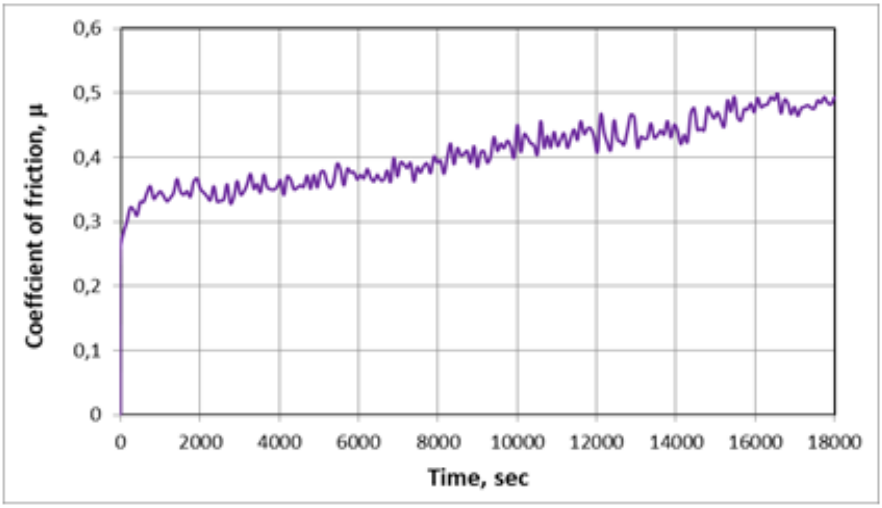

Figure 15. Evolution of the friction coefficient for sample A10/25.

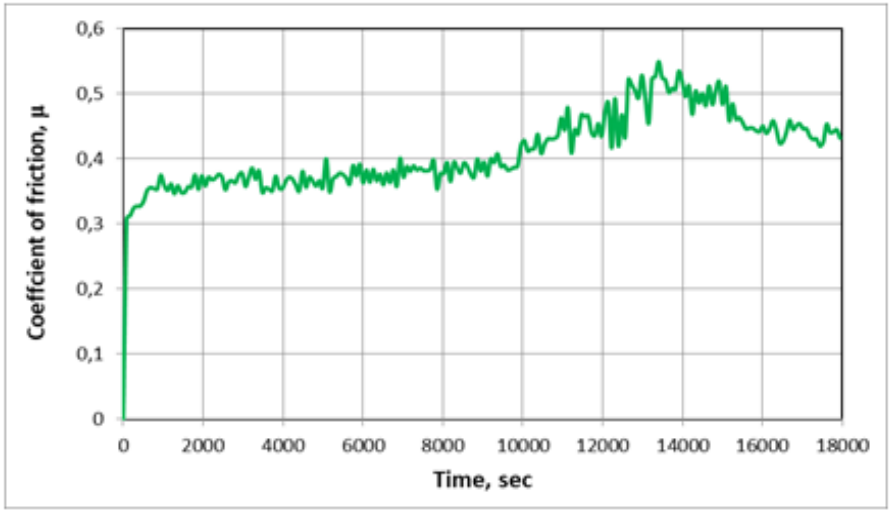

Figure 16. Evolution of the friction coefficient for sample A15/20.

Generally, the friction coefficient stabilized after an interval of 14,000 seconds from the start of the tests. For sample A5/30, the friction coefficient stabilized around 0.53, for sample A10/25 around 0.48, and for sample A15/20 around 0.45.

The highest friction coefficient value recorded for the A5/30 sample is due to its high stiffness and low porosity, which favors intense contact with the brake disc.

3.2. DISCUSSION

The A5/30 sample is characterized by a rigid and brittle behavior, manifested by high hardness, low porosity, and high compressive strength, but low resilience. A higher proportion of SRB introduced in the A10/25 sample results in a beneficial compromise between hardness and toughness. Thus, the elastomeric phase increases energy absorption capacity and resilience, without excessively reducing strength properties. At even higher concentrations (A15/20), an amplification of elastic phenomena is observed, increasing resilience and elongation at break, in parallel with a decrease in hardness and compressive

strength. This effect is aggravated by the increase in porosity and the reduced interfacial adhesion between the rubber particles and the phenolic matrix.

Of the samples analyzed, the A10/25 material presents the best overall mechanical behavior for brake pad application. It achieves an optimal compromise between hardness, compressive strength, and resilience, offering a favorable combination of structural rigidity and energy absorption capacity.

Table 7 shows that the wear of cast iron is lower than that of composite materials. The highest relative wear durability is the A15/20 sample. In this recipe, there is a relatively balanced proportion between rubber and wood dust. This is due to the balance between SRB rubber and wood dust, which provides stable tribological behavior. The elastomeric phase reduces contact stresses and absorbs shocks, while the wood particles stabilize friction by forming a protective surface film.

The combination of these effects leads to uniform wear and an increase in the durability of the friction material. Wear resistance is a useful parameter for estimating brake pad life [14]. A low wear rate implies better wear resistance, and in this context, the most wear-resistant material is A15/20. This behavior is due to the optimal ratio between SRB and wood dust, which ensures the formation of a stable tribological film, shock absorption, and a uniform distribution of contact stresses. The increase in rubber content has resulted in reduced abrasive wear and microcracking, while the moderate proportion of wood helps to stabilize friction and maintain the integrity of the surface layer. In contrast, stiffer and more brittle materials (A5/30) exhibit a higher wear rate due to the lack of an elastic phase capable of dissipating friction energy.

The highest temperature in the contact area of the friction couplings was recorded for sample A5/30, due to the high friction and the lack of an elastic phase capable of dissipating thermal energy. The rigid and brittle material favors heat accumulation and rapid temperature increase on the surface. In contrast, sample A15/20 presents the best overall thermal stability due to the higher content of SRB rubber, which dampens thermal shocks, reduces local stress concentrations, and promotes uniform heat dissipation in the composite mass. This balanced structure gives the material stable thermal behavior during the braking process. During the tests, the temperatures recorded in the contact area did not exceed 180°C. Mentioning this aspect is very important, as the component materials of the analyzed recipes present thermal behavior thresholds above which irreversible degradation processes occur. In the range of 180–200°C, depolymerization of SRB rubber occurs, a phenomenon that causes loss of elasticity and modification of mechanical properties [16]. Wood dust undergoes thermal transformations in the range of 200–250°C, manifested by carbonization and loss of structural integrity [15].

Therefore, friction materials developed and tested in the laboratory are recommended for use in braking systems of small, medium-performance urban vehicles, where thermal stresses remain below these critical thresholds.

Sample A10/25 presents a moderate but more stable friction coefficient, due to the balance between rigid and elastic phases (Fig.15). The A15/20 sample, although it has a slightly lower coefficient, benefits from the best stability and durability, thanks to the elasticity of the SRB rubber and the formation of a protective tribological film (Fig. 16).

The specialized literature specifies values of friction coefficients for friction materials within a fairly wide range of values. Practically, for most vehicles, the nominal values of friction coefficients vary between the limits of 0.3-0.6 [18]. The friction coefficients obtained for the materials tested in this study fall within the previously specified limits.

4. CONCLUSIONS

It can be concluded that *(i)* analyzing the mechanical behavior of the analyzed recipes, it is observed that increasing the proportion of SRB rubber decreases stiffness and strength, but increases deformation capacity and energy absorption; *(ii)* from a tribological point of view, a moderate to high content of SRB rubber increases the stability of the friction coefficient and reduces wear, while rigid materials provide high but unstable and more aggressive friction for the disc; *(iii)* analyzing thermal behavior, increasing the proportion of rubber reduces temperature peaks and improves thermal stability, protecting the material structure during braking; *(iv)* A5/30 has high hardness and friction coefficient, but low resilience and rapid wear; *(v)* A10/25 offers an optimal balance between hardness, resilience, tribological and thermal stability, being the most suitable for urban applications; *(vi)* A15/20 provides maximum resilience and energy absorption, reduced wear and superior thermal stability, but lower stiffness and hardness limit performance under heavy braking; *(vii)* using rubber particles and wood dust in brake pads proves to be a smart strategy for a circular economy; *(viii)* the proposed material is a viable, sustainable, and efficient alternative for light braking applications.

REFERENCES

[1] Garett, T. K., Newton, K., Steeds, W., *The Motor Vehicle*, 13th Ed., Society of Automotive Engineers, Warrendale, Pennsylvania, 902, 2001.
[2] Limpert, R., *Brake Design and Safety*, 2nd Ed., Society of Automotive Engineers, Warrendale, Pennsylvania, 8, 1999.
[3] Patnaik, A., *Tribology in Materials and Manufacturing - Wear, Friction and Lubrication*, Ed. IntechOpen, 120, 2021.
[4] Ciudin, R., Verma, P.C., Gialanella, S., *The Sustainable City IX*, **2,** 1423, 2014.
[5] Stojanovic, N., Glisovic, J., Abdullah, O. I., Belhocine, A., Grujic, I., *Environmental Science and Pollution Research*, **29**, 9606, 2022.
[6] Seo, H., Joo, B., Park, J., Kim, Y. C., Lee, J. J., Jang, H., *Tribology International*, **154**, 106713, 2021.
[7] Tamayo, A., Rubio, F., Pérez-Aparicio, R., Saiz-Rodríguez, L., Rubio, J., *Polymers*, **13**(19), 1, 2021.
[8] Imran, A. L. I., Siregar, J. P., Mat Rejab, M. R., Cionita, T., Hadi, A. E., Jaafar, J., Fitriana, D. F., Dewi, R., *Special Issue on Technology*, **4**(3), 337, 2024.
[9] Dirisu, J. O., Okokpujie, I. P., Josep, O. O., Oyedepo, S. O., Falodun, O., Tarbitu, L. K., Shehu, F. D., *Journal of Renewable Materials*, **12**(3), 1, 2024.
[10] Wang, N., Liu, H., Hung, F., *Lubricants*, **11**(1), 27, 2023.
[11] Kurniawan, M. A., Prasetyo, I., Fahmagi, A. E., Turasno, B., Development of Brake Pads from Teak Wood Powder and Rice Husk Ash using Hotpress, *2nd International Conference on Environment, Green Technology, and Digital Society*, **622**, 01007, 2025.
[12] Nandiyanto, A. B. D., Fitriani, A. F., Pradana, R. A., Ragadhita, R., Azzaoui, K., Piantari, E., *Moroccan Journal of Chemistry*, **12**(2), 714, 2024.
[13] Dirisu, J. O., Okokpujie, I. P., Apiafi, P. B., Oyedepo, O. S., Tartibu, L.K., Omotosho, A. O., Ogunkolati, O. E., Oyeyemi, E. O., Uwaishe, J. O., *Journal of Engineering and Applied Science*, **71**(55), 1, 2025.

[14] Tamayo, A., Rubio, F., Perez-Aparicio, R., Saiz-Rodriguez, L., Rubio, J., *Polymers*, **13**(19), 1, 2021.
[15] Mutlu, I., Sugözü, I., Keskin, A., *Polymers*, **25**, 440, 2015.
[16] Li, Z. X., Kong, Y. R., Chen, X. F., Huang, Y. J., Lv, Y. D., Li, G. X., *Chinese Journal of Polymer Science*, **41**, 1287, 2023.
[17] Pascu, L., *Research on improving the quality of brake shoes for rolling stock*, Doctoral thesis, University Politehnica Timișoara, 93, 2014
[18] Anderson, A. E., *Friction and wear of automotive brakes*, Materials Park, OH. ASM Handbook, 18, 1992.